

# Subwavelength resolved terahertz real-time imaging based on a compact and simplified system

Zhiyong Tan (谭智勇)<sup>1,2\*</sup>, Wenjian Wan (王文坚)<sup>1</sup>, Chang Wang (王长)<sup>1,2</sup>, and Juncheng Cao (曹俊诚)<sup>1,2\*\*</sup>

<sup>1</sup>Laboratory of Terahertz Solid-state Technology, Shanghai Institute of Microsystem and Information Technology, Chinese Academy of Sciences, Shanghai 200050, China

<sup>2</sup>Center of Materials Science and Optoelectronics Engineering, University of Chinese Academy of Sciences, Beijing 100049, China

\*Corresponding author: [zytan@mail.sim.ac.cn](mailto:zytan@mail.sim.ac.cn)

\*\*Corresponding author: [jccao@mail.sim.ac.cn](mailto:jccao@mail.sim.ac.cn)

Received March 27, 2022 | Accepted May 17, 2022 | Posted Online June 10, 2022

A real-time imaging system based on a compact terahertz laser is constructed by employing one off-axis parabolic mirror and one silicon lens. Terahertz imaging of water, water stains, leaf veins, human hairs, and metal wire is demonstrated. An imaging resolution of 68  $\mu\text{m}$  is achieved. The experiments show that this compact and simplified imaging system is suitable for penetration demonstration of terahertz light, water distribution measurement, and imaging analysis of thin samples.

**Keywords:** terahertz; real-time imaging; subwavelength resolution; compact laser.

**DOI:** [10.3788/COL20220.091101](https://doi.org/10.3788/COL20220.091101)

## 1. Introduction

Terahertz real-time imaging is a promising technology for applications in material characterizations, material reaction analysis, and biomedical imaging<sup>[1,2]</sup>. The first, to the best of our knowledge, demonstration of real-time imaging in terahertz region was realized by employing a powerful gas laser<sup>[3]</sup>. However, the gas laser is huge and expensive, which makes it difficult to obtain practical application in the imaging system. Therefore, Lee *et al.*<sup>[4]</sup> developed an imaging system by employing the quantum-cascade laser (QCL) that is one of the important terahertz solid-state sources with high output power and compact structure. After that, research on terahertz real-time imaging has been rapidly developed in the past ten or more years<sup>[5–14]</sup>. By improving the performance of terahertz arrays<sup>[5,8]</sup>, the real-time imaging demonstration with a resolution of hundreds of microns is realized. Using a microscope lens and synchronous signal locking, the imaging resolution is improved to less than 100  $\mu\text{m}$ <sup>[6]</sup>. Finally, a two-dimensional wobbling mirror has been used to eliminate the interference fringes of the emitting light of terahertz QCL<sup>[11]</sup>. Although the performance and imaging effects of terahertz real-time imaging systems have been greatly improved by employing the above improvements in receiver and optical path, the complex optics and high cost make the above imaging system unable to be widely used.

In this Letter, a simplified and low-cost imaging system is built by employing a compact terahertz laser (QCL) and simplified optics, in which, one off-axis parabolic (OAP) mirror and one silicon lens have been used and fixed on a vertical guide rail.

The terahertz transmission images of two human hairs and a metal wire are acquired by employing a thermal array with a high-density polyethylene (HDPE) window. The imaging resolution is analyzed, and subwavelength resolved imaging has been obtained.

## 2. Experiment

The emitted light from compact terahertz QCL is collected and collimated by an  $f/1$  OAP mirror with a focal length of 50.8 mm. After passing through the sample plate, the collimated terahertz light is focused on a thermal array by a silicon lens with a diameter of 38.1 mm and a focal length of 50 mm. The schematic of the real-time imaging system is shown in Fig. 1. The terahertz QCL has the same active region and fabrication process as in Ref. [15]. The emission wavelength of the laser is 70  $\mu\text{m}$  (4.28 THz).

In this experiment, a 3 mm  $\times$  100  $\mu\text{m}$  terahertz QCL with an output power about 1.5 mW at 60 K is used. The device is fixed on the cold finger of a little Stirling refrigerator with a cooling power about 2 W at 60 K. The laser is driven by a customized high-power pulse generator, with a voltage amplitude of 15 V, a repetition rate of 20 kHz, and a duty cycle of 8%. A high-resistance silicon (HRSi) lens is used for gathering the imaging light. The front and rear surfaces of the lens are evaporated with the antireflection film to reduce the reflection loss. A 1-mm-thick HDPE window is used to filter out most of the background radiation in the infrared region, and then most of the transmission light can pass through the window and reach the thermal

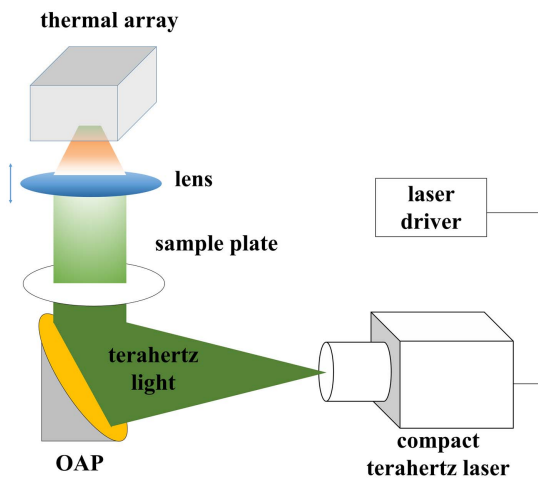


Fig. 1. Schematic of the real-time imaging system with a compact terahertz laser.

array with a pixel size of  $17\ \mu\text{m}$  and pixels of  $384 \times 288$ . The noise equivalent power (NEP) of the thermal array is calibrated to about  $200\ \text{pW}/\text{Hz}^{1/2}$  at  $70\ \mu\text{m}$ . The frame rate is set to 25 Hz. During imaging, the sample is placed on a 1-mm-thick HDPE plate with a transmittance of more than 90% at  $70\ \mu\text{m}$ . The HDPE plate is placed horizontally and perpendicular to the imaging light. A translation stage with a vertical traveling length of 10 mm and a moving accuracy of  $10\ \mu\text{m}$  is used to move the silicon lens accurately.

### 3. Experimental Results and Discussion

The real-time transmission imaging of the water on an HDPE sample cell was demonstrated to verify the performance of this imaging system. The red frame shown in Fig. 2(a) represents the area of imaging with a frame rate of 25 Hz. The imaging data is processed by the Origin software by Contour mode with the number of the level set to 60, the intensity scale set to log, and the label increment of the color bar set to 10 (the following images are processed in the same way). The color of the processed image is set to black and white, and the image is shown in Fig. 2(b), in which the black areas indicated by the white arrows represent weak signal results from being absorbed by water. In Fig. 2(b), the water in the center cell and the water

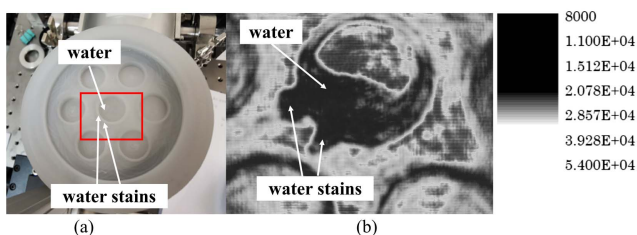


Fig. 2. (a) Optical and (b) terahertz images of water and water stains on an HDPE sample cell.

stains on the edge of the cell are clearly shown. The above demonstration provides a good verification for real-time imaging of liquid.

In order to verify the penetration characteristics of this  $70\ \mu\text{m}$  light in imaging, the real-time transmission imaging of a dried bamboo leaf on an HDPE sample plate was demonstrated with the same frame rate. The red frame shown in Fig. 3(a) represents the area of imaging. The color of the processed image is set to rainbow, and the image is shown in Fig. 3(b), in which the edge of the leaf is very clear, and the leaf veins can be obviously distinguished.

Then, the real-time transmission imaging of two human hairs and a metal wire (bent into number eight) was carried out with the same frame rate. The color of the processed image is set to black and white, and the image is shown in Fig. 4(b). Figure 4(a) shows its optical image. In the terahertz image, the hairs and metal wire are clearly shown. Two crossed hairs are clearly distinguished. It should be noted that there is stripe diffraction noise in Fig. 4(b), which is mainly due to the non-uniform light from terahertz QCL, resulting in different degrees of diffraction effects when quasi parallel terahertz light passes through the sample and in pattern noise intertwined with the shape of the sample in the thermal array. In addition, due to the long wavelength of the terahertz laser, the strip spot will be generated when emitting from the ridge facet of terahertz QCL, resulting in a fringe noise signal in the terahertz image. The above situation is particularly obvious when the signal-to-noise ratio (SNR) is poor.

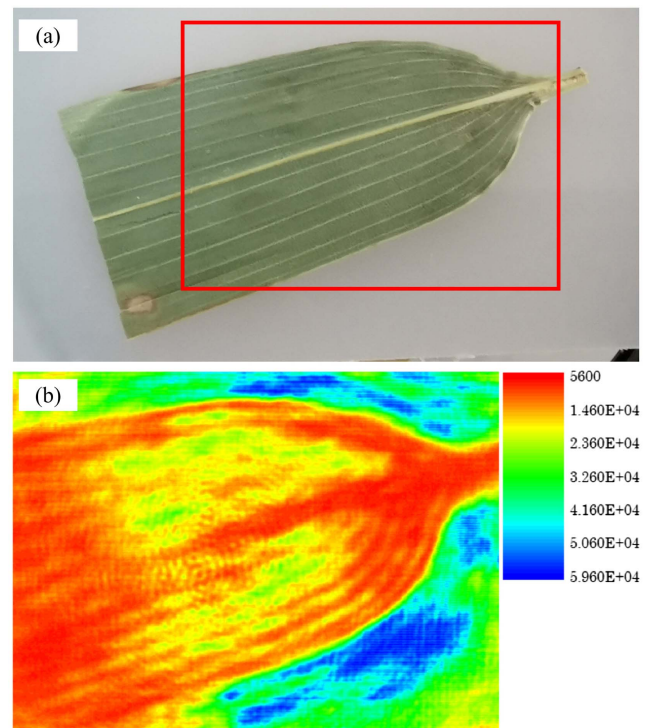


Fig. 3. (a) Optical and (b) terahertz images of a dried leaf on an HDPE sample plate.

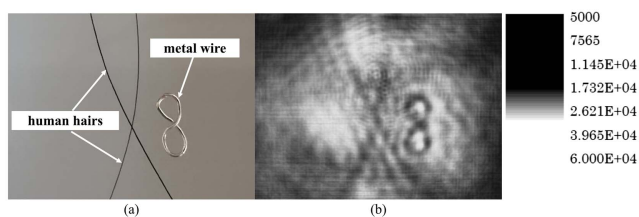


Fig. 4. (a) Optical and (b) terahertz images of two human hairs and a metal wire [bent into number eight].

To obtain the imaging resolution, another imaging experiment of the above samples is conducted. The silicon lens fixed on the one-dimensional translation stage is moved finely to get a clearer image of the human hairs. At this point, the terahertz image of the metal wire does not accurately match to the sensitive surface of the thermal array, so the image line of the metal wire becomes thicker than that in Fig. 4(b). In order to estimate the spatial resolution of this imaging system, the color of the processed image is set to black and white, and the image is shown in Fig. 5(b); the transmission amplitude of a cross section at pixel line 103 (the red short dashed line) in the image is drawn in Fig. 5(a). Due to the poor light beam quality of terahertz QCL, it is difficult to meet the Gaussian or flattened Gaussian distribution. Therefore, we choose full width at half-minimum (FWHM) as a threshold to estimate the spatial resolution. From Fig. 5(a), at the best resolution, there are only four pixel intervals. In other words, the best imaging resolution is  $17\ \mu\text{m} \times 4 = 68\ \mu\text{m}$ , which indicates that the resolution size is smaller than the laser wavelength. The diameter, with a value of about  $60\ \mu\text{m}$ , of the hair has also been measured by a micrometer. The results acquired by employing our compact imaging system provide a proof-of-concept demonstration; however, the imaging quality should be improved in further work, such as a terahertz QCL with better beam quality and higher energy conversion efficiency as the light source in our system. Furthermore, a liquid nitrogen dewar may be used for cooling the terahertz QCL in order to reduce the cost of the system.

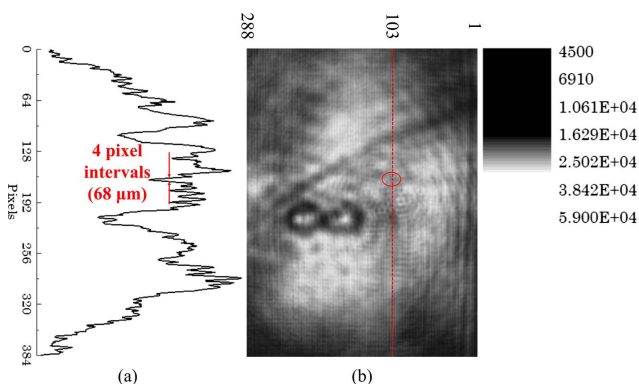


Fig. 5. (a) Transmission amplitude of a cross section of the terahertz image in (b); the red short dashed line indicates the detailed location.

## 4. Conclusion

In summary, we have demonstrated real-time imaging based on a compact terahertz laser and simplified optics. Terahertz images of water, water stains, leaf veins, human hairs, and metal wire have been acquired. An imaging resolution of  $68\ \mu\text{m}$  has been obtained, in which a subwavelength resolved imaging performance is shown. The results show that our compact and simplified imaging system is suitable for penetration demonstration of terahertz light, water distribution measurement, and imaging analysis of thin samples. To obtain a clearer image with higher SNR, a terahertz laser with better beam quality and higher energy conversion efficiency must be used. The SNR of the system may be improved by employing a dry air inflation structure, and a liquid nitrogen dewar may be used for further reducing the cost of the system in further work.

## Acknowledgement

This work was supported by the National Natural Science Foundation of China (Nos. 61927813, 61975225, and 62035014) and Science and Technology Commission of Shanghai Municipality (Nos. 21DZ1101102 and 21ZR1474600).

## References

1. M. Tonouchi, "Cutting-edge terahertz technology," *Nat. Photonics* **1**, 97 (2007).
2. Z. Y. Tan, W. J. Wan, H. Li, and J. C. Cao, "Progress in real-time imaging based on terahertz quantum-cascade lasers," *Chin. Opt.* **10**, 68 (2017).
3. A. W. M. Lee and Q. Hu, "Real-time, continuous-wave terahertz imaging by use of a microbolometer focal-plane array," *Opt. Lett.* **30**, 2563 (2005).
4. A. W. M. Lee, B. S. Williams, S. Kumar, Q. Hu, and J. L. Reno, "Real-time imaging using a 4.3-THz quantum cascade laser and a  $320 \times 240$  microbolometer focal-plane array," *IEEE Photon. Technol. Lett.* **18**, 1415 (2006).
5. N. Oda, H. Yoneyama, T. Sasaki, M. Sano, S. Kurashina, I. Hosako, N. Sekine, T. Sudoh, and T. Irie, "Detection of terahertz radiation from quantum cascade laser, using vanadium oxide microbolometer focal plane arrays," *Proc. SPIE* **6940**, 69402Y (2008).
6. N. Oda, T. Ishi, T. Morimoto, T. Sudou, H. Tabata, S. Kawabe, K. Fukuda, A. W. M. Lee, and Q. Hu, "Real-time transmission-type terahertz microscope with palm size terahertz camera and compact quantum cascade laser," *Proc. SPIE* **8496**, 84960Q (2012).
7. A. W. M. Lee, Q. Qin, S. Kumar, B. S. Williams, and Q. Hu, "Real-time terahertz imaging over a standoff distance ( $>25$  meters)," *Appl. Phys. Lett.* **89**, 141125 (2006).
8. Z. Y. Tan, L. Gu, T. H. Xu, T. Zhou, and J. C. Gao, "Real-time reflection imaging with terahertz camera and quantum cascade laser," *Chin. Opt. Lett.* **12**, 070401 (2014).
9. N. Oda, A. W. M. Lee, T. Ishi, I. Hosako, and Q. Hu, "Proposal for real-time terahertz imaging system with palm-size terahertz camera and compact quantum cascade laser," *Proc. SPIE* **8363**, 83630A (2012).
10. A. Bergeron, M. Terroux, L. Marchese, O. Pancrati, M. Bolduc, and H. Jerominek, "Components, concepts, and technologies for useful video rate THz imaging," *Proc. SPIE* **8544**, 85440C (2012).
11. N. Oda, T. Ishi, S. Kurashina, T. Sudou, M. Miyoshi, T. Morimoto, T. Yamazaki, T. Tsuboi, and T. Sasaki, "Palm-size and real-time terahertz imager, and its application to development of terahertz sources," *Proc. SPIE* **8716**, 871603 (2013).

12. S. Z. Fan, F. Qi, T. Notake, K. Nawata, Y. Takida, T. Matsukawa, and H. Minamide, "Diffraction-limited real-time terahertz imaging by optical frequency up-conversion in a DAST crystal," *Opt. Express* **23**, 7611 (2015).
13. F. Simoens, J. Meilhan, and J.-A. Nicolas, "Terahertz real-time imaging uncooled arrays based on antenna-coupled bolometers or fet developed at CEA-leti," *J. Infrared Millim. Te.* **36**, 961 (2015).
14. R. I. Stantchev, X. Yu, T. Blu, and E. Pickwell-MacPherson, "Real-time terahertz imaging with a single-pixel detector," *Nat. Commun.* **11**, 2535 (2020).
15. Z. Y. Tan, H. Y. Wang, W. J. Wan, and J. C. Cao, "Dual-beam terahertz quantum cascade laser with >1 W effective output power," *Electron. Lett.* **56**, 1204 (2020).